ELSEVIER

Thermochimica Acta 304/305 (1997) 291–301

thermochimica acta

Character of the phase transition in liquid crystals by AC calorimetry

M. Castro*, J.A. Puértolas

Dpto Ciencia de Materiales. Centro Politécnico Superior – ICMA, Universidad de Zaragoza – C.S.I.C., 50015 Zaragoza, Spain

Received 7 August 1996; accepted 4 April 1997

Abstract

A method based on the analysis of the temperature sensor of a high-resolution AC calorimeter has been developed in order to determine the character of the phase transition in liquid crystals. A comparative study between this method, denoted as 'thermistor method', and the standard phase shift procedure is carried out in different kind of liquid crystal phase transitions. The sensitivity of the standard phase shift method has been studied through the thermal models for our system. Finally, the method, when it is applied to first-order transitions, provides additional thermal features as coexistence region, metastability and latent heat ratio between transitions, and it could allow to elucidate the assignment of the character of the transition lines in phase diagrams. © 1997 Elsevier Science B.V.

Keywords: AC calorimetry; Liquid crystals; Phase transition character

1. Introduction

During the last twenty years, AC calorimetry has been shown as a powerful tool in order to study phase transitions and critical phenomena in liquid crystals.

Although the first measurement by AC calorimetry was made in 1910 by Corbino [1], it is only after 1967, with Sullivan and Seidel [2], when the low temperature range and the modelling of the thermal link effects were considered. Finally, it was near 1980 when several groups (Smaardyk, Johnson, Huang and Garland [3–6]) started to investigate liquid crystal samples which had a very low thermal conductivity, and where very slow internal thermal equilibrium was expected. An extensive review of classical AC calorimetry and its development is explained by Gmelin in this same issue.

AC calorimetry has several useful advantages for the study of phase transitions, since the measurements are performed near thermal equilibrium with a good resolution for small heat-capacity changes, even with a small amount of sample. A high-temperature resolution close to the critical temperature is also reached. Hysteresis effects can be studied since cooling and warming measurements are possible and, finally, non adiabatic conditions are required. These advantages allow to compare the thermodynamic theories and aspects of the liquid crystal phase transitions (mean-field behaviour, critical fluctuation models, location of multicritical points on binary mixtures and character of phase transition) [7,8] with the experimental data.

The most important handicap of this technique is the impossibility to quantitatively determine the latent

*Corresponding author. Fax: 0034-76-761957; e-mail: miguel.-castro@mcps.unizar.es.

PII S0040-6031(97)00176-7

heat of the first-order transitions, although some attempts to determine it indirectly have appeared [9,10]. However, the first-order character of a phase transition is detected by this technique through an anomalous change in the phase shift between the heating power and the temperature oscillation [7].

In this work, we describe an alternative method, namely, the 'thermistor method', in order to analyse the character of the liquid crystal phase transitions by AC calorimetry. The method is tested and compared with the phase shift method through several examples of different liquid crystal transitions.

2. Set up and thermophysical models

Specific heat measurements have been performed on a high-resolution AC calorimeter for liquid crystals and solid samples, in the temperature range 30–250°C, which is described elsewhere [11]. It is based on a previous one described in the literature [7], but some modifications were introduced in order to improve its versatility and resolution.

The schematic diagram of the experimental installation is shown in Fig. 1 and can be followed while we review briefly its principal features. The source of the modulated input power is a strain gauge which operates as a resistive heater (R=120 Ω) and as sample support. Solid samples are glued directly over the heater while silver home made or DSC aluminium capsules are used for liquid samples. Typically 5–50 mg of sample are needed. The sensor for detecting the temperature oscillations is glued in the opposite face of the sample and it is a microbead thermistor (1–3 MΩ at room temperature) supplied by a high stability home-built DC current supply. A lock-in amplifier (EG&G model 5302), which permits to extend the frequency range down to 1 mHz, acts as an oscillator for the heater and also measures the AC voltage and phase shift generated in the thermistor. The mean temperature of the sample is determined from the sampling of the thermistor voltage in some periods with a HP3457A digital voltmeter. Finally, the heater–sample–sensor assembly is surrounded by two concentric copper blocks, where vacuum can be made or helium can be introduced in order to control the thermal link with the surroundings. The whole system is immersed into a thermostatic bath equipped with a temperature controller which allows to scan the temperature slowly with different rates, from 0.5 to 5 K/h.

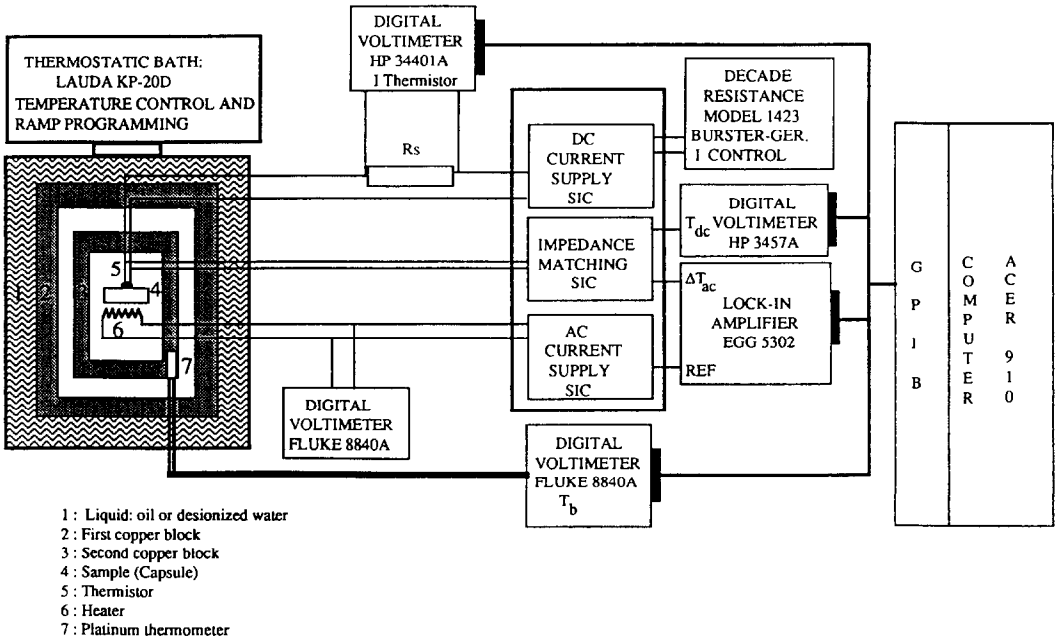

Fig. 1. Schematic diagram of the high-resolution AC calorimeter.

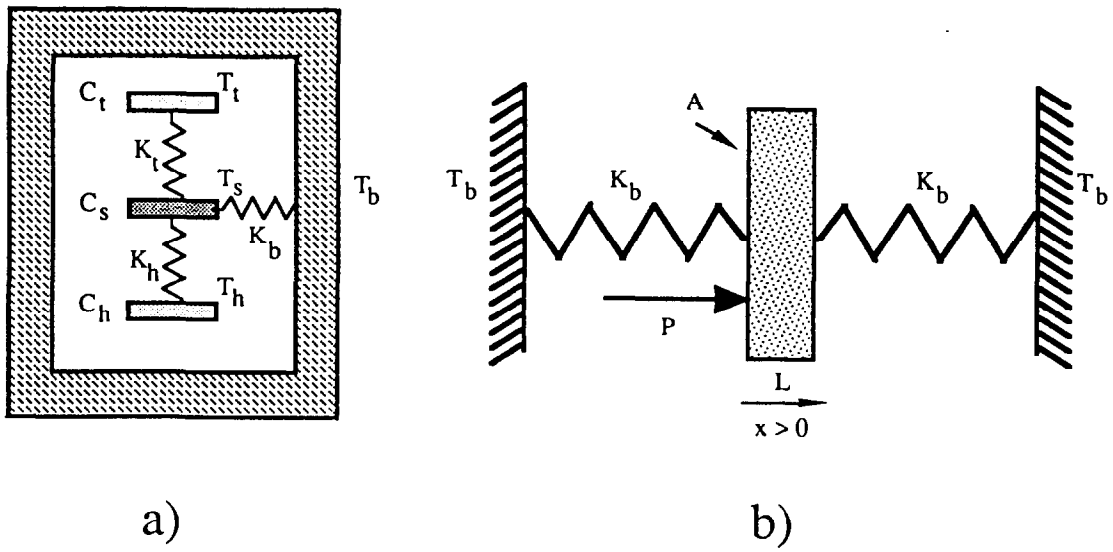

Fig. 2. Thermal models. (a) A heater and thermometer, with heat capacities C_h and C_t, respectively, are connected to the sample (or capsule) by thermal conductance K_h, K_t. The sample has a heat capacity C_s. The whole assembly is loosely connected to the copper block, at temperature T_b, by a conductance K_b, (b) One-dimensional model in order to take into account the thermal conductivity of the sample. An ideal thermal contact between heater, thermometer and sample is considered. The sample can exchange heat from both faces to the surroundings, through two equal thermal conductances K_b.

Measurements performed on samples like 4-*n*-octyloxy-4′-cyanobiphenyl (8OCB), cyanobenzylidene-*p*-*n*-octyloxyaniline (CBOOA) liquid crystals and the ferroelectric triglicine sulfate (TGS) compound [11,12] have allowed to estimate the absolute and relative accuracy, which are around 5 and ±0.1%, respectively. The critical behaviour observed on these samples were in agreement with that reported in the literature.

In this work, we have studied theoretically two thermal models that reflect our physical system. The first one, represented in Fig. 2(a), consists of a heater and thermometer connected to the sample (or capsule) by thermal conductance K_h, K_t and with heat capacities C_h and C_t, respectively. The sample has a heat capacity C_s. The whole assembly, with total heat capacity $C = C_t + C_h + C_s$ is loosely connected to the copper block, at temperature T_b, by a conductance K_b. We assume that the sample, thermometer and heater have infinite thermal conductivity. If the sample is going out of equilibrium, some relaxation constants can be defined. One is the time required by the system to reach equilibrium with the surrounding block, $\tau_s = C/K_b$, called external relaxation time, and the others are the internal times $\tau_t = C_t/K_t$, $\tau_h = C_h/K_h$, which correspond to the time needed by the thermometer and heater in order to reach equilibrium with the sample.

Considering a sinusoidal heating power, $P = P_0 \cos^2(\omega t/2)$, the amplitude and phase shift of the temperature oscillation for this thermal system, studied by Seidel and Sullivan [2], can be solved. The temperature detected by the thermometer is:

$$T_t = T_b + \Delta T_{DC} + \Delta T_{AC} \cos(\omega t - \alpha) = T_b + \frac{P_0}{2K_b} + \frac{P_0}{2\omega C} G \cos(\omega t - \alpha) \quad (1)$$

where G and the phase shift α are the complex functions of the frequency, heat capacities, thermal conductances and time constants.

This temperature have two interesting terms: A DC step, $\Delta T_{DC} = P_0/2K_b$, above the block temperature, T_b, and a sinusoidal temperature oscillation which will allow to obtain the heat capacity. If $\omega\tau_t$ y $\omega\tau_h < 1$ and $\omega\tau_s > 1$, the amplitude of the oscillation temperature, ΔT_{AC}, and the phase shift can be simplified up to first

order on $\omega^2(\tau_t^2 + \tau_h^2)$, and $(\omega\tau_s)^{-2}$:

$$\Delta T_{AC} = \frac{P_0}{2\omega C}\left[1 + \frac{1}{\omega^2\tau_s^2} + \omega^2(\tau_t^2 + \tau_h^2)\right]^{-\frac{1}{2}}$$

$$\text{and } \cot\alpha = \frac{1}{\omega\tau_s} - \omega(\tau_h + \tau_t) \qquad (2)$$

Additionally, we propose in order to take into account the finite thermal conductivity of the sample, k, a one-dimensional model corresponding to the scheme in Fig. 2(b).

In this model, a sample of density ρ, specific heat c, thickness L and surface $A(A \gg L)$ is heated on one face by a power $P = (P_0/2A)e^{i\omega t}$, and a perfect thermal contact between the sample, heater and thermometer is assumed. Additionally, the sample can exchange heat with the surroundings from both faces as is indicated by two equal thermal conductances, K_b. In this case with the condition $\omega\tau_s > 1$ where $\tau_s = C_s/2K_b$, and $L < l_0$, with $l_0 = (2a/\omega)^{1/2}$, the amplitude of the temperature oscillation is [12]:

$$\Delta T_{AC} = \frac{P_0}{2\omega C_s}\left[1 + \frac{1}{\omega^2\tau_s^2} + 2\sqrt{10}\frac{\tau_{int}}{\tau_s} + \left(1 + \sqrt{\frac{45}{8}}\frac{\tau_{int}}{\tau_s}\right)\omega^2\tau_{int}^2\right]^{-\frac{1}{2}} \qquad (3)$$

where $\tau_{int} = L^2/a\sqrt{90}$ is the internal thermal relaxation time of the sample and $a = k/\rho c$ is the thermal diffusivity. Therefore, the presence of a finite thermal conductivity of the sample introduces a frequency dependent term similar to that obtained in the first model for the thermometer and heater.

Considering both the models and if the conditions are largely satisfied, the frequency dependent terms are negligible and the expressions for calculating the heat capacity of the sample and the phase take the form:

$$\Delta T_{AC} = \frac{P_0}{2\omega C} \text{ with } \alpha \approx \frac{\pi}{2}. \qquad (4)$$

In our set up the external relaxation time is typically around 50 s and the internal relaxation time due to the thermal conductivity of the liquid crystal is around 1 s. These values give a corrective term of around 1–4% in C_p.

In order to select a frequency which allows to use the simplified expression for determining the heat capacity, frequency scans at constant block temperature and power are performed. Typical representations of this frequency response are shown in Fig. 3. The first corresponds to a plot ΔT_{AC} versus ω^{-1} (3a), which must show a region with a linear dependence and the second, log-log plot of $\omega\Delta T_{AC}$ versus ω (3b), must show a frequency plateau. The narrow region determined through both the representations corresponds to the adequate frequency range where the

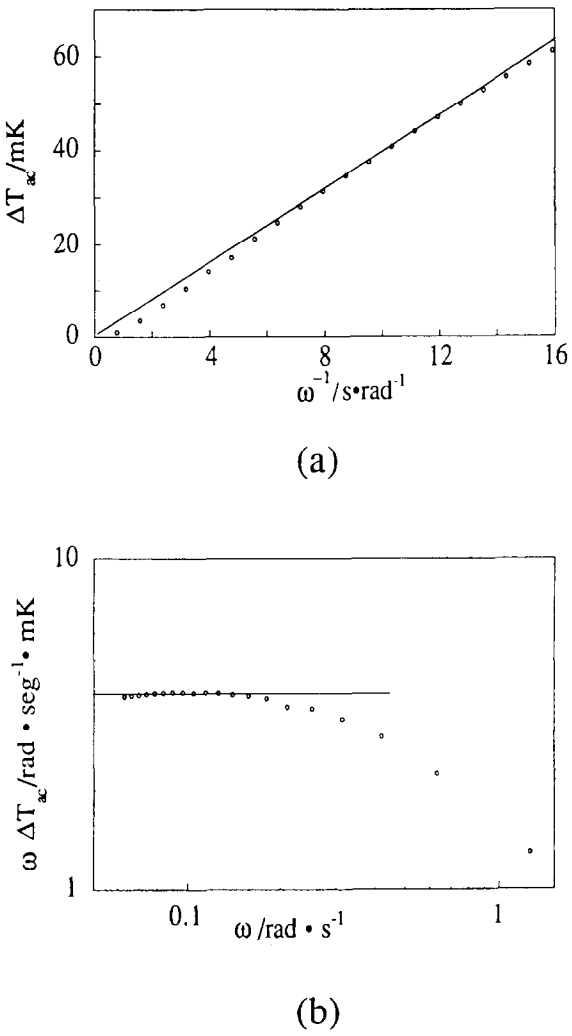

Fig. 3. Frequency response at constant temperature. (a) ΔT_{AC} vs. ω^{-1}. (b) $\omega\Delta T_{AC}$ vs. ω. The linear region and the plateau area correspond to the adequate frequency range where the measurement can be done and the simplified expression (4) for the heat capacity can be used.

measurement can be performed and the simplified expression for the heat capacity can be used.

3. Thermistor method

The usual method to determine the character of a transition in AC calorimetry is the analysis of the thermal hysteresis. Its existence indicates first-order transition while its absence is not conclusive. However, some liquid crystals often show a drift in the transition temperatures with time (for instance, 10 mK/day and 80 mK/h [13,14]) which prevents the evaluation of the thermal hysteresis. Only the comparison between several heating and cooling processes allows to do some corrections in order to delimit the thermal hysteresis.

An intrinsic method of the AC calorimetry is the measurement of changes in the phase shift [7]. Usually, the occurrence of a first-order transition can be detected by an abrupt increase in the value of the phase shift, α, and also in the heat capacity, C_p. Typically, there is a peak in α almost coincident with a detected apparent heat capacity peak. For a second-order transition, the phase shift generally shows a smooth dip with a minimum at a temperature corresponding to the maximum of C_p. Sometimes, changes in the phase shift are not detected for this kind of transition [15].

We have developed an alternative procedure, denoted as 'thermistor method' to study the character of the phase transition using a high-resolution AC calorimeter with a highly sensitive temperature sensor. The bases for this method are the following: Let us suppose that an ideal linear temperature heating or cooling ramp is programmed to the block by means of the thermostatic bath. The DC component of the thermistor temperature (mean-temperature), T_{tm}, should follow this linear scan over the whole temperature range. However, when the sample passes through a first-order transition, the latent heat absorbed or released by the sample induces an anomalous thermal variation of T_{tm} from its expected behaviour. This effect is remarkable because the thermistor has a small mass and heat capacity, a good thermal contact with the sample or the sample holder and finally its resistance has a high-temperature coefficient. These features allow to detect a small latent heat by means of the anomalous variation of the DC temperature of the thermistor.

The evaluation of this thermal deviation from the ideal expected linear behaviour is the basis of our method. For doing this, the DC expected thermistor temperature in the transition region, T^*_{tm}, is calculated from the linear interpolated curve of the DC thermistor temperature in two temperature ranges away from the transition (below and above). The difference between the measured DC sample temperature (T_{tm}) and the interpolated temperature (T^*_{tm}) is denoted by ΔT and plotted against T^*_{tm}. This calculation does not use the block temperature and therefore avoids the bath temperature fluctuations (±5 mK at 343 K as the best case). Bath fluctuations are higher than the thermistor ones, due to the additional damping obtained with the vacuum surrounding the inner copper block. A value of $\Delta T \neq 0$ ($\Delta T < 0$ on heating and $\Delta T > 0$ on cooling) means that some latent heat exists in the transition and a first-order character can be assigned.

However, some departures from the above ideal case can appear. Sometimes one of the temperature ranges, above or below the transition, can be affected by another transition or by a non-linear behaviour of the programmed ramp due to the influence of the thermostatic bath. In this case, T^*_{tm} is calculated extrapolating the linear fit of T_{tm}, obtained in the other range where the linearity exists. In this case, ΔT will also be different from zero outside the transition and the deviation of ΔT with respect to this smooth departure from the linearity has to be taken into account. Then, on heating through a first-order transition the thermistor undergoes a cooling with respect to the smooth behaviour whereas on cooling the thermistor will heat up with respect to this smooth behaviour. These deviations indicate the presence of latent heat. Some of the examples shown through this paper correspond to this situation.

4. Liquid crystal samples

Specific heat measurements, shown in this paper, have been carried out on different samples. Some of the results correspond to the mixtures of two isomers: 4-octyloxyphenyl 4′-decyloxybenzoate (10OPEPO8) and 4-decyloxyphenyl 4-octyloxybenzoate (8OPEPO10). The synthesis and elemental analysis

are described in Ref. [16]. The antiferroelectric liquid crystal (R)-1-methylheptyl 4-(4″-decyloxybenzoyl-oxy)-biphenyl-4-carboxylate (MHDOBBC) was synthesized using commercially available (S)-(+)-2-octanol (Aldrich) which served as enantiomerically enriched starting material. Information about the esterification reaction, purification process and the analysis of the chemical structure are described in Ref. [17].

5. Comparison between phase shift and thermistor methods

In this section, we have studied the behaviour of each method in some phase transitions with different character. We will start with the first-order character, following with the second order and finally, we apply the method through a weak first-order transition which has a low enthalpy content. In this context we will analyse the limitations of both methods in order to distinguish the transition character.

5.1. First-order transitions

The melting from the crystalline solid to the fluid or to a mesophase is not an important transition in the work done on liquid crystals by calorimetry. Moreover, its first-order character permits to compare both phase shift and thermistor method.

We have chosen the melting transition from the crystal to the SmC phase for the 10OPEPO8-8OPEPO10 binary mixture with 40% of 8OPEPO10 [16,18]. The measurement has been carried out at 10 mHz, a scan rate of 1 K/h and with sample mass of 5.6 mg. The results obtained in the first heating are shown in Fig. 4(a) and indicate that a large peak is presented with a maximum at 329.88 K, in agreement with the onset at 329 K of the peak measured by DSC done at 0.5°C/min. In the same figure, the phase shift is represented and a strong increase occurs in the same temperature region where a large and apparent heat capacity is detected. The width of this region is 5.5 K which corresponds to the phase conversion temperature range. Thermal gradients, imperfections and impurities can increase the size of this region.

In Fig. 4(b), the same transition is represented together with the magnitude ΔT corresponding to

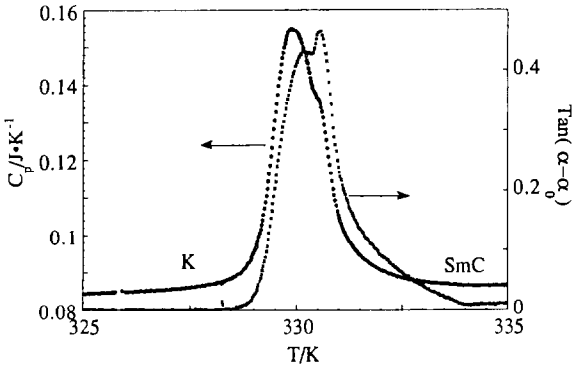

(a)

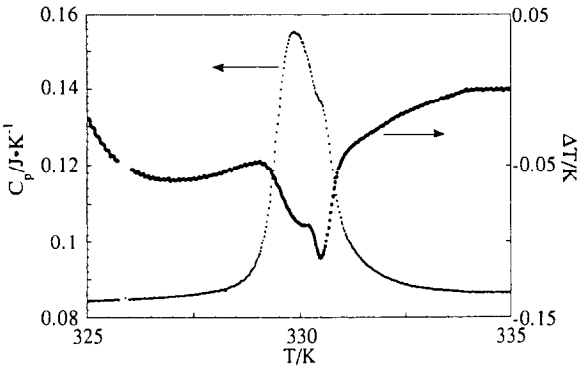

(b)

Fig. 4. Melting transition for the 10OPEPO8-8OPEPO10 binary mixture with 40% of 8OPEPO10. (a) (○) Heat capacity, (x) phase. (b) (•) Same heat capacity, (●) ΔT.

the thermistor method. A large and sharp deviation with respect to the smooth behaviour appears in the same temperature region than the heat capacity peak and phase shift anomaly, proving the same origin for both signatures. The peak on ΔT indicates that the sample absorbs heat from its surrounding and of course from the thermistor. The presence of a second anomaly in C_p as a hump at 330.5 K, suggests that the sample undergoes two sequential first-order transitions. Both phase shift and ΔT show two anomalies. This first-order sequence is also detected by DSC.

The nematic–isotropic transition (N–I) is expected to have a weak first-order character, according to the mean field in the Landau–de Gennes model [19]. In

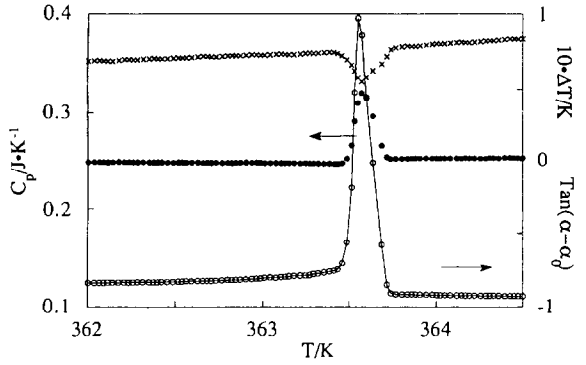

Fig. 5. Nematic–Isotropic (N–I) transition for the compound 10OPEPO8. (○) Heat capacity, (●) phase and (x) $10\times\Delta T$.

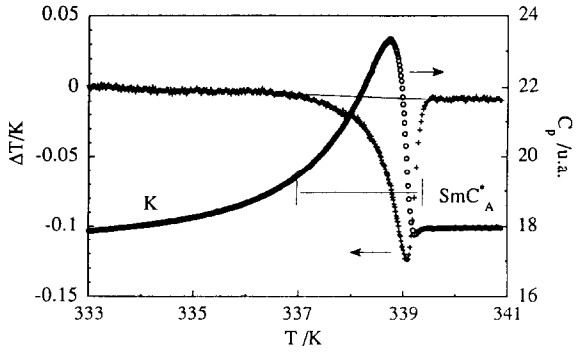

Fig. 6. Melting transition for the MHDOBBC liquid crystal. (○) heat capacity and (+) ΔT. The vertical arrows indicate the phase coexistence region.

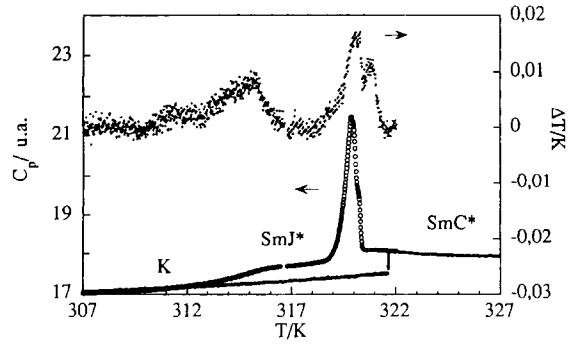

Fig. 7. Heat capacity (○) obtained on cooling the MHDOBBC liquid crystal. (+) ΔT. (●) C_p during a quench-and-hold experiment at 321.4 K during 24 h followed by a cooling process.

Fig. 5, we represent the N–I transition for the pure compound 10OPEPO8 on heating it at 1 K/h, 10 mHz and for 4 mg of sample mass. A sharp peak at 363.25 K is detected. In this case, a two-phase coexistence region of 0.2 K wide can be delimited also by a change or kink in the heat capacity behaviour. The sharp peak of the phase shift and ΔT, coincident with the observed heat capacity anomaly, corroborates this temperature range and the first-order nature.

In both the transitions, we have made evident that the new method is comparable to the phase shift method for a strong first-order character. As a consequence of the validity of the method, we can apply it to determine some features of the first-order transitions. So, we can estimate and separate the temperature range where the phase coexistence takes place from the range where pretransitional effects on C_p are predominant. An example of this behaviour corresponds to the measurement of the melting transition (K–SmC$^*_A$) for the MHDOBBC liquid crystal [20] obtained under the conditions of 15 mHz, a scan rate of 1 K/h and an amount of 23 mg of sample. The results of C_p and ΔT are depicted in Fig. 6 and the vertical arrows point out the temperature range (around 2 K) where $\Delta T \neq 0$ and where the K and SmC$^*_A$ phases coexist. Therefore, the rest of the region where an excess of heat capacity is observed corresponds to the pretransitional or fluctuation region. Similar behaviour has been determined in the melting transition of the MHPOCBC [21] liquid crystal.

A second application can be shown through the cooling process of the MHDOBBC sample, which is plotted in Fig. 7. A large peak in C_p appears at 319.82 K corresponding to the freezing of the SmC$^*_A$ to SmJ* and additionally there is a stepwise behaviour at lower temperature which indicates a recrystallization process. The results of ΔT shows two anomalies associated to both phenomena. However, lowering the temperature and prior to the anomaly related with the SmC$^*_A$–SmJ* phase transition, a peak on ΔT is observed in a region where the heat capacity is almost constant. This feature indicates the metastability of the SmC* phase and that the freezing starts during the SmC$^*_A$ cooling process. The latent heat released in the freezing process increases the thermistor temperature. This metastable behaviour was confirmed by means of a quench-and-hold experiment at 321.4 K during 24 h followed by a cooling process which is also shown in the same figure.

The last feature is concerned with the determination of the latent heat relation between different first-order

transitions of the same compound. So, we have compared the latent heats between the freezing of the SmC_A^* and the melting transition which have been scanned over with the same rate. Since the temperature range where $\Delta T \neq 0$ is the same in both, it means that a similar conversion rate takes place. In this condition, the maximum value of ΔT, ΔT_{max}, will be proportional to the latent heat. The value for the ΔT_{max} are 0.017 and 0.12 K, respectively, giving a value ratio of 0.14. The enthalpy contents determined by DSC for these transitions are ΔH=4.2 and 31.7 kJ/mol, respectively. The enthalpy ratio is 0.13, practically equal to the ΔT_{max} ratio.

5.2. *Second-order transition.*

We have concentrated on our comparative study of the SmC (SmC*)–SmA phase transitions which usually have second-order character in agreement with the de Gennes model prediction [19]. However, this model classifies this transition in the three-dimensional XY universality class while the experimental results can be described within the framework of the extended mean-field theory [7,8,14,22,23]. Recently, certain compounds have shown a non-mean field behaviour above the critical temperature [24,25]. On the other hand, some liquid crystals with high spontaneous polarization have been shown to exhibit first-order SmC*–SmA transitions [26–28].

First-order transition SmC–SmA can exist on a binary system with an NAC point if the location of the tricritical point is displaced from the NAC one, so that the second-order SmA–SmC line changes to a line of first-order character. This behaviour seems to be influenced by some physical parameter like the size of the SmA temperature range [28,29], high spontaneous polarization at the SmC* phase [28,30,31], large molecular dipole moments [32] and the nematic range [23].

In this context, we are studying the 10OPEPO8-8OPEPO10 binary mixture [16,18] whose phase diagram is represented in Fig. 8, where the NAC point is located at around and less than 60% of 8OPEPO10 and the SmC-N line has a first-order character. For the pure compound 10OPEPO8, the C_p data corresponding to the SmC–SmA transition are represented in Fig. 9, showing the typical shape for a mean field behaviour. In Fig. 9(b) the ΔT is represented together with the

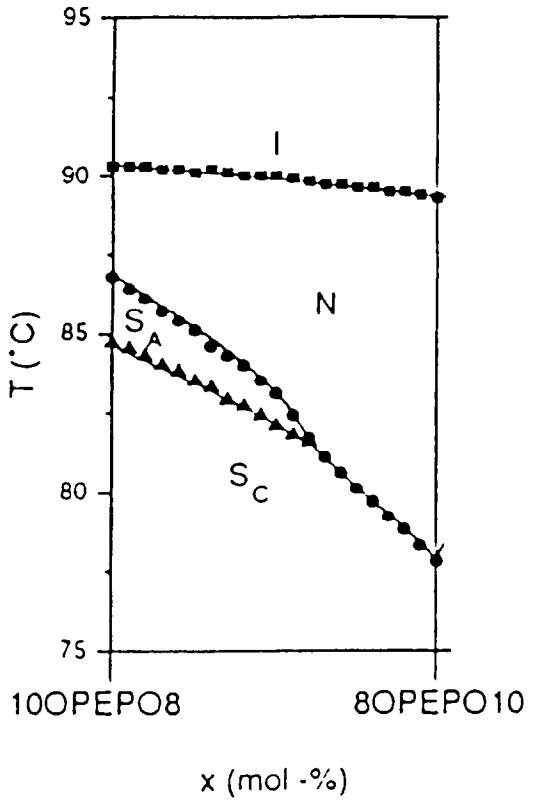

Fig. 8. Phase diagram of the 10OPEPO8-8OPEPO10 binary mixture.

heat capacity. The absence of any effect on ΔT allows to point out the absence of latent heat and characterize the transition as a second order one. However, the result of the phase shift plotted simultaneously in Fig. 9(a) has a dip or smooth decrease, when we must expect any variation of the phase shift in accordance with the expressions (4).

In order to explain the existence of a dip in this kind of transition, we have estimated the temperature dependence of the phase in the framework of the thermal models, taking into account the fact that the terms depending on the thermal conductivity are negligible for the selected frequency. The procedure is the following: with the simplified expression (3) of the oscillation amplitude, we estimate τ_s=30 s by fitting a frequency response at a temperature near the transition. The $\alpha(T)$ is calculated using the simplified phase expression (3), the estimated value of τ_s, the experimental heat capacity, C_p, and the operating frequency,

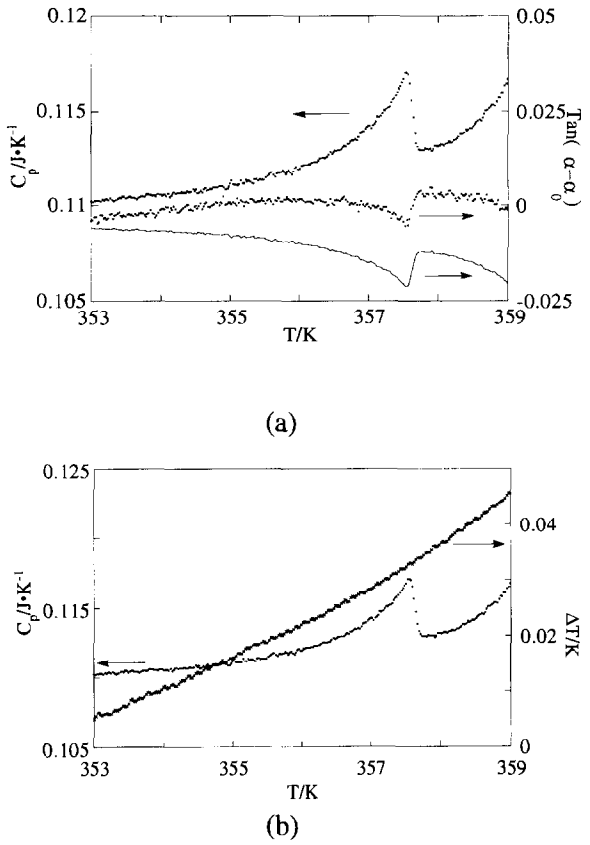

Fig. 9. SmC–SmA phase transition for the compound 10OPEPO8. (a) (x) heat capacity, (•) phase. (-) simulation of the phase as is explained in the text. (b) (o) same heat capacity, (x) ΔT.

ω_0. A dip appears in the calculated result, which is represented as a continuous line in Fig. 9(a). The calculation also indicates that the dip is strongly frequency dependent. In fact, an increase of ω_0 would smooth the effect and even revoke the dip. However, this ideal frequency can not be achieved experimentally due to the influence of the terms depending on the thermal conductivity of the sample.

From the former results, we could think that the thermistor method present an advantage respect to the assignment of the transition character, since no changes are detected on ΔT during the transition, while α show a dip. However, a simple analysis allows to estimate also some limitations to the thermistor method. The thermal equation which describe the sample temperature, T, when the bath temperature, T_B, increases linearly with the time at the scan rate, m, $T_B = T_0 + mt$, is the following:

$$C_p \frac{dT}{dt} = K_B(T_B - T) = K_B(T_0 + mt - T) \quad (5)$$

where T_0 is the initial temperature of the bath. The sample temperature when a stationary state is obtained is:

$$T = mt + T_0 - \frac{C_p}{K_B} m \quad (6)$$

The sample temperature must show a lag in temperature, $-(C_p/K_B)m$, proportional to the heat capacity and the scan rate. If the heat capacity changes over the transition, this temperature lag will change and will affect ΔT. For example, for the first-order transition on Fig. 4, the change on the temperature lag due to the increase of the heat capacity would be around 10 mK. In this case, this value is lower than the experimental value of ΔT=80 mK, indicating the presence of latent heat.

Therefore both methods present departures from the ideal conditions. For the phase shift method the non-ideal selected frequency generate a dip and for the thermistor one an excessive scan rate induce a detectable variation on ΔT. In both the cases high values of C_p increase these effects and establish limits for the application of these methods as we will see subsequently.

The presence of a dip on the phase shift must not be necessarily related with a second-order character. So, the N–SmC transition for the binary system on Fig. 8 with 60% of 8OPEPO10 located near but on the right side of the NAC point, present a weak first-order transition with a low latent heat. The weak first-order character of this transition for our dilution has been confirmed by volumetric measurements [18]. The heat capacity measurement obtained on cooling at 2 K/h, 10 mHz and with 4 mg of sample are represented in Fig. 10. The phase shift shows a small dip (Fig. 10a), while ΔT, represented on Fig. 10(b), shows an increase when the transition occurs. The existence of a dip on the phase shift could be explained through the expression (3) and following the same procedure used for the second-order transition SmC–SmA analysed previously. The calculated phase shift, with τ_s=30 s, is represented by a continuous line on Fig. 10(a) and shows a dip clearly larger than the experimental one. As a consequence of this analysis,

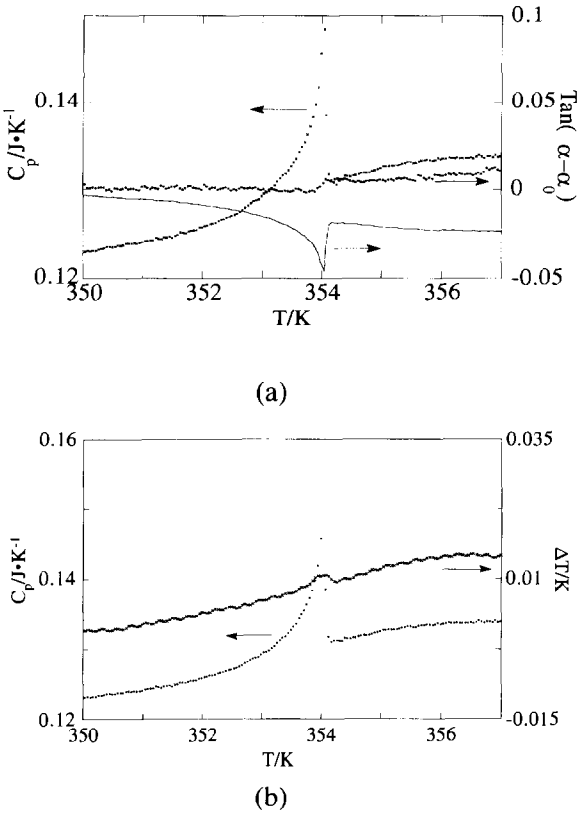

Fig. 10. SmC–N phase transition for the 10OPEPO8-8OPEPO10 binary mixture with 60% of 8OPEPO10. (a) (x) Heat capacity, (●) phase and (—) simulation of the phase as is explained in the text. (b) (○) Same heat capacity, (x) ΔT.

we consider that two contributions for the phase shift could be present in a weakly first-order transition. One of them associated to the non-ideal operating frequency and the other to the latent heat which acts in the opposite sign. The first effect could mask the second one and even become predominant. This last behaviour could drive to an erroneous second-order assignment to this N–SmC transition in accordance to the existence of a dip.

The increase of ΔT must indicate that a latent heat is present in this transition in agreement with the volumetric measurements. However, a careful analysis of ΔT must be done in this transition since the increase of the heat capacity as well as the selected scan rate can induce a detectable change on the temperature lag and can give an influence on ΔT. The estimated change, with τ_s=30 s, would be around 2.3 mK in agreement with the experimental value. Therefore this contribution can be due to the heat capacity change and scan rate and not to the presence of latent heat. Measurement at a lower scan rate has been done in order to observe the evolution of ΔT. However, the result obtained at 1 K/h indicate that the scan rate is not low enough in order to distinguish both contributions.

This general analysis could help us to understand the phenomenology reported in other compounds [33] with respect to the phase transition character assignment, taking into account the limitations of both methods when the character of the phase transition is weak first order.

6. Conclusions

A method to determine the transition character in liquid crystals, denoted as 'thermistor method' has been introduced. The comparison performed between this method and the usual phase shift, it is noted that both methods present a comparable sensitivity in the strong first-order transitions. The thermistor method has been applied to study some features related with the coexistence range, metastability, and latent heat ratio in first-order transitions as mesophase-isotropic or crystal-mesophase. Additionally, both methods have been tested and discussed on a second-order transition and its limitations has been analysed through a weak first-order transition.

Acknowledgements

We wish to thank Dr. D. Guillon and Dr. B. Heinrich for providing some of the liquid crystal samples measured in this work.

References

[1] O.M. Corbino, Phys. Z., 11 (1910) 413.
[2] P.F. Sullivan and G. Seidel, Phys. Rev., 173 (1968) 679.
[3] J.E. Smaardyk and J.M. Mochel, Rev. Sci. Instrum., 49 (1978) 988.
[4] D.L. Johnson, C.F. Hayes, R.J. deHoff and C.A. Schantz, Phys. Rev. B, 18 (1978) 4902.
[5] C.C. Huang, J.M. Viner, R. Pindak and J.W. Goodby, Phys. Rev. Lett., 46 (1981) 1289.

[6] C.W. Garland, G.B. Kasting and K.J. Lushington, Phys. Rev. Lett., 43 (1979) 1420.
[7] C.W. Garland, Therm. Acta, 88 (1985) 127.
[8] C.W. Garland, Phase Transition in Liquid Crystal, Plenum Press, New York, 1992, Chap. 11.
[9] I. Hatta, H. Ichikawa and M. Todoki, Therm. Acta, 267 (1995) 83.
[10] P.R. Garnier and M.B. Salamon, Phys. Rev. Lett., 27 (1971) 1523.
[11] M. Castro and J.A. Puértolas, J. Therm. Analys., 41 (1994) 1245.
[12] M. Castro, PhD. Thesis, University of Zaragoza, Spain, 1995.
[13] X. Wen, C.W. Garland and M.D. Wand, Phys. Rev. A, 42 (1990) 6087.
[14] J. Boerio-Goates, C.W. Garland and R. Shashidhar, Phys. Rev. A, 41 (1990) 3192.
[15] G.S. Iannacchione and D. Finotello, Phys. Rev. E, 50 (1994) 4780.
[16] B. Heinrich, PhD. Thesis, University Louis Pasteur of Strasbourg, France, 1993.
[17] Y. Gónzalez, PhD. Thesis, University of Zaragoza, 1995.
[18] M. Castro, J.A. Puértolas, B. Heinrich, D. Guillon. Calorimetric and dilatometric study on a binary liquid crystal system. 16th International Liquid Crystal Conference, University of Kent, USA 1996. Poster C2P.11, P-145.
[19] P.G. de Gennes, The Physics of Liquid Crystals, Clarendon, Oxford, 1974.
[20] J.A. Puértolas, M. Castro, M.R. de la Fuente, M.A. Pérez Jubindo, H. Dreyfus, D. Guillon and Y. Gónzalez, Mol. Cryst. Liq. Cryst., 287 (1996) 69.
[21] K. Ema, H. Yao, I. Kawamura, T. Chan and C.W. Garland, Phys. Rev. E, 47 (1993) 1023.
[22] M. Meichle and C.W. Garland, Phys. Rev. A, 27 (1983) 2624.
[23] J. Zubia, M. Castro, J.A. Puértolas, J. Etxebarria, M.A. Pérez-Jubindo and M.R. de la Fuente, Phys. Rev. E, 48 (1993) 1970.
[24] L. Reed, T. Stoebe and C.C. Huang, Phys Rev. E, 52 (1995) 2157.
[25] K. Ema, J. Watanabe, A. Takagi and H. Hao, Phys. Rev. E, 52 (1995) 1216.
[26] Ch. Bahr and G. Heppke, Mol. Cryst. Liq. Cryst., 150b (1987) 313.
[27] B.R. Ratna, R. Shashidhar, G.G. Nair, S.K. Prasad, Ch. Bahr and G. Heppke, Phys. Rev. A, 37 (1988) 1824.
[28] R. Shashidhar, B.R. Ratna, G.G. Nair, S.K. Prasad, Ch. Bahr and G. Heppke, Phys. Rev. Lett., 61 (1988) 547.
[29] C.C. Huang and S.C. Lien, Phys. Rev. A, 31 (1985) 2621.
[30] G. Heppke, D. Lotzsch and R. Shashidhar, Liq. Cryst., 5 (1989) 489.
[31] H.Y. Liu, C.C. Huang, Ch. Bahr and G. Heppke, Phys. Rev. Lett., 61 (1988) 345.
[32] H.Y. Liu, C.C. Huang, T. Min, M.D. Wand, D.M. Walba, N.A. Clark, Ch. Bahr and G. Heppke, Phys. Rev. A, 40 (1989) 6759.
[33] X. Wen, C.W. Garland, R. Shashidhar and P. Barois, Phys. Rev. B, 45 (1992) 5131.